Physica C 475 (2012) 38–42

Contents lists available at SciVerse ScienceDirect

Physica C

journal homepage: www.elsevier.com/locate/physc

Influence of different pinning ability on harmonic susceptibilities in high-temperature superconductors

L. Zhang [a,b,*], S.Y. Ding [b], G.H. Liu [a], P. Li [a], Z. Tang [a], Y.B. Li [a], K. Huang [a], X.B. Zhu [c], Y.P. Sun [c]

[a] Department of Mathematics and Physics, Anhui University of Architecture, Hefei 230022, People's Republic of China
[b] National Laboratory of Solid State Microstructures, Department of Physics, Nanjing University, Nanjing 210093, People's Republic of China
[c] Key Laboratory of Materials Physics, Institute of Solid State Physics, Chinese Academy of Science, Hefei 230031, People's Republic of China

ARTICLE INFO

Article history:
Received 30 September 2011
Received in revised form 2 January 2012
Accepted 25 January 2012
Available online 7 February 2012

Keywords:
Harmonic susceptibilities
Flux pinning
Sintered superconductors

ABSTRACT

Influence of flux pining ability in the intragrain characterized by critical current density on the harmonics AC susceptibility is studied. A sintered superconducting sample is described by alternating weak (intergrains or weak links) and strong (intragrains) regions, which is depicted by different critical current densities J_{cw} and J_{cs}. Simulations using the flux creep model show that with the increase of the flux pinning ability of the intragrain region, a step and two peaks in the fundamental AC susceptibility as well as more peaks in the higher order even and odd harmonics are observed. Moreover, the Coles–Coles plot of χ_3 may be used as a method to qualitatively estimate the values of J_{c0s}/J_{c0w}.

1. Introduction

The behaviors of high-temperature superconductors (HTSCs) under the external magnetic fields are considered important due to their engineering applications. Several techniques have been applied to study the complicated flux motions of HTSCs under the varying temperatures and fields, such as transport, magnetization, and AC susceptibility [1–4]. In particular, the complex AC susceptibility ($\chi_n = \chi'_n + i\chi''_n$) has been widely used to study the vortex dynamics and loss mechanism of HTSCs. It is well known that a measurement of the fundamental AC susceptibility ($\chi_1 = \chi'_1 + i\chi''_1$) represent two complementary aspects of flux dynamics: just below the critical temperature T_c, a sharp decrease in the real part χ'_1 is a consequence of diamagnetic shielding and a peak in the imaginary part χ''_1 represents losses [5,6]. In addition to the fundamental response χ_1, the higher order harmonics are usually generated in HTSCs owing to the non-linear flux creep. This nonlinear response of the superconductors to a change in the external magnetic field is studied carefully [7,8]. Experimentally, the higher order harmonics have been widely used as an accurate and sensitive method to define the irreversible line and non-linear dissipation [9–11]. Additionally, the higher order harmonic response is more sensitive to the extern parameters and sample properties [12,13].

As to the large scale applications of HTSCs, it is crucially dependent on their critical current density (J_c) and irreversibility field. A sintered sample of HTSCs consists of superconducting grains, which are interconnected by a system of weak links. The existence of weak links sensitively affects on the higher order harmonics.

Lots of works have been made to explain higher order harmonics by considering a sample consisting of the intergrain and intragrain components in sintered HTSCs [1–3,13,14]. However, the systematic investigation of different flux pinning ability effects on higher order harmonics is still lack. Moreover, the size of the weak links also significantly influent of higher order harmonics. Therefore, the investigation is necessary to get a picture of the higher order harmonics influenced by the flux pinning and the size of intragrain.

In previous works, the critical state model has been used to explain experimental results about higher order harmonics [15,16]. For HTSCs, flux creep is significant due to the high operating temperatures and small activation energy U. Hence, flux creep models are used in the study of higher order harmonics [17,18]. In order to reach a fundamental understanding of higher order harmonics in the sintered HTSCs, in this paper, we propose a phenomenological model to describe the sintered HTSCs and to study the effects of flux pinning and the size of intragrain on higher order harmonics.

2. Simulation

For a sintered sample of HTSCs, the grain boundaries (intergrain) form a weak link network of flux pinning, which suppresses substantially the critical current density, and thus contains a lower

* Corresponding author at: Department of Mathematics and Physics, Anhui University of Architecture, Hefei 230022, People's Republic of China. Tel.: +86 551 3828233; fax: +86 551 3828133.
E-mail address: lizhang@aiai.edu.cn (L. Zhang).

0921-4534/$ - see front matter © 2012 Elsevier B.V. All rights reserved.
doi:10.1016/j.physc.2012.01.015

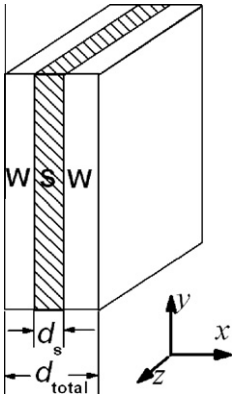

Fig. 1. A schematic sketch of the one-dimensional model: a superconducting slab consisting of periodic strong part (the intragrain) and weak part (intergrain).

J_c, whereas the intragrain region has a higher J_c. As magnetic field is applied, flux density will enter into the intergrain at first and then penetrate gradually into the intragrain by means of flux creep. Hence, a sintered sample is simplified by a 'sandwich' of an intragrain region (S) with higher J_c by two intergrain regions (W) with lower J_c, as shown in Fig. 1, which is similar to the two velocity hydrodynamic models [8,23].

Consider a slab with infinite length along the y axis, thickness d along the x axis, and width w along the z axis. The field is applied along the z axis. In view of $w \gg d$,we focus on the one-dimensional case for simplicity [19,20]. The nonlinear flux diffusion is described by the logarithmic barrier, $U(j) = U_0 \ln |j_c/j|$ [19,20], and thus the flux line velocity is

$$v = v_0(j/j_c)\exp[-U(j)/kT] = v_0(j/j_c)|j/j_c|^n, \tag{1}$$

where $n = U_0/(\mathrm{kT})$ and v_0 is the velocity at $U = 0$. For simplification, we suppose $U_{0w} = U_{0s} = U_0$. Let the surfaces of the slab be in y–z plane, thickness d along the x axis, the applied field $B_a \| z$. Using the Maxwell equations, one gets the diffusion equation of flux line

$$\frac{\partial B}{\partial t} = \frac{v_0}{(\mu_0 J_c)^{n+1}}\frac{\partial}{\partial x}\left[\left|\frac{\partial B}{\partial x}\right|^n\left(\frac{\partial B}{\partial x}\right)|B|\right]. \tag{2}$$

The boundary and initial conditions are, respectively,

$$B(x = 0, d; t) = B_{dc} + B_{ac}\sin(2\pi ft),$$

$$B(x; t = 0) = B_{dc}.$$

The complex elementary ACS then can be calculated by

$$\chi_n = \chi_n' + i\chi_n'' = \frac{1}{\pi B_{ac}}\int_0^{2\pi}\mu_0 M(t)\exp(in2\pi ft)d(2\pi ft), \tag{3}$$

where the magnetization is

$$\mu_0 M(t) = \left[\frac{1}{d}\int_0^d B(x,t)dx\right] - [B_{dc} + B_{ac}\sin(2\pi ft)]. \tag{4}$$

The temperature and field dependence of the critical current density and apparent activation energy are supposed as follows, respectively,

$$j_c(T,B) = j_{c0}\left[1 + \left(\frac{T}{T_c}\right)^2\right]^{-1/2}\left[1 - \left(\frac{T}{T_c}\right)^2\right]^{5/2}\frac{B_0}{B_0 + |B|}, \tag{5}$$

$$U_0(T,B) = U_{00}\left[1 - \left(\frac{T}{T_c}\right)^4\right]\frac{B_0}{B_0 + |B|}, \tag{6}$$

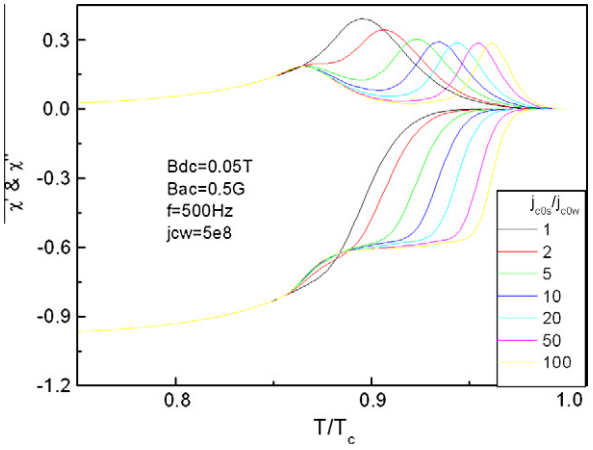

Fig. 2. The calculated curves of χ_1' and χ_1'' as a function of temperature with different J_{c0s}/J_{c0w}, as the arrows indicate: 1, 2, 5, 10, 20, 50, 100, for $B_{dc} = 0.05$ T, $B_{ac} = 0.5$ Gs and $f = 500$ Hz.

In the following simulations, we let $n_0 = n(T = 0, B = 0) = 5$, $v_0 = 1$ m/s

and $B_0 = 500$ Gs [18]. On the other hand, we choose $j_{c0w} = 5 \times 10^8$ A/m^2 and j_{c0s} is several times larger than j_{c0w}. With the finite difference method, the nonlinear diffusion equation can be numerically solved and the implicit difference scheme is used for stability.

3. Results and discussion

Firstly, we focus on the influence of flux pinning on complex susceptibility. Hence, that the intragrain zone holds 2/9 part of the whole sample, and the other 7/9 part is intergrain zone has been choose [20]. Additionally, the higher J_c means stronger flux pinning [21], so we adapt J_c value reflect the flux pinning ability. In Fig. 2, we plot the calculated curves of χ_1' and χ_1'' as a function of temperature at $B_{dc} = 0.05$ T, $B_{ac} = 0.5$ Gs and $f = 500$ Hz, for various values of J_{c0s}/J_{c0w} (1, 2, 5, 10, 20, 50, and 100). As the values of J_{c0s}/J_{c0w} increase, one peak in χ_1'' becomes two peaks, and smooth increase of χ_1' from -1 to 0 appears a step as temperature goes up, which is in good agreement with experimental data [3].

The calculated higher order even and odd harmonics as a function of temperature at $B_{dc} = 0.05$ T, $B_{ac} = 0.5$ Gs and $f = 500$ Hz are presented in Figs. 3 and 4, respectively. Solid lines and dished lines indicate the real part and imaginary part of higher harmonics, respectively. The simulated results are also in agreement with experiments [3,12,15]. The real and imaginary part of higher order harmonics oscillate between positive and negative values, seen from Figs. 3 and 4. As the values of J_{c0s}/J_{c0w} increase from 1 to 100, in the real parts of higher order even harmonics, the peak positions move towards to higher temperatures, and the peak heights increase, shown in Fig. 3. The previous studies indicate that an observation of even harmonics means the existence of an asymmetric hysteresis loops with magnetic fields between $B_{dc} + B_{ac}\sin(2\pi ft)$ and $B_{dc} + B_{ac}\sin(2\pi ft + \pi)$ [22]. It means that the asymmetry of minor hysteresis loops becomes obviously as flux pinning ability increasing of strong region. In Fig. 4, similar peaks as in even harmonics versus temperature curves can be observed, however, it is noted that the peak heights decrease as the increment of flux pinning ability.

In order to show the influence of flux pinning ability on the harmonics clearly, we plot in Figs. 5 and 6 the magnitude of the odd ($|\chi_3|$, $|\chi_5|$, $|\chi_7|$, $|\chi_9|$) and even ($|\chi_2|$, $|\chi_4|$, $|\chi_6|$, $|\chi_8|$) harmonics, where $|\chi_n| = \sqrt{\chi_n'^2 + \chi_n''^2}$, as a function of temperature at $B_{dc} = 0.05$ T, $B_{ac} = 0.5$ Gs, and $f = 500$ Hz, for various values of

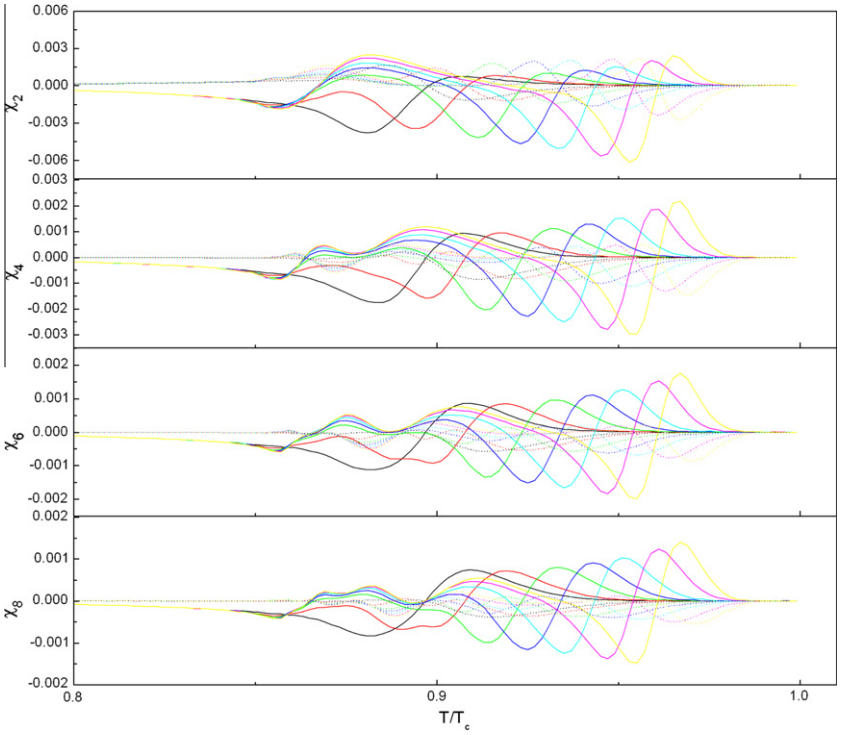

Fig. 3. The calculated curves of even hamonics χ_n' and χ_n'' (n = 2, 4, 6, 8) as a function of temperature with different J_{c0s}/J_{c0w}, as the arrows indicate: 1, 2, 5, 10, 20, 50, 100, for B_{dc} = 0.05 T, B_{ac} = 0.5 Gs and f = 500 Hz.

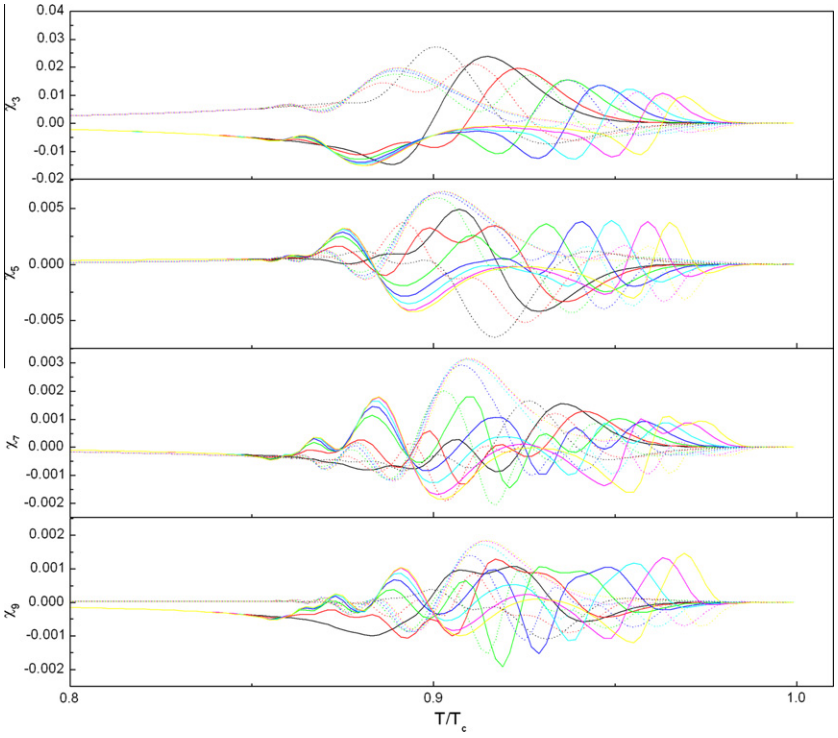

Fig. 4. The calculated curves of odd hamonics χ_n' and χ_n'' (n = 3, 5, 7, 9) as a function of temperature with different J_{c0s}/J_{c0w}, as the arrows indicate: 1, 2, 5, 10, 20, 50, 100, for B_{dc} = 0.05 T, B_{ac} = 0.5 Gs, and f = 500 Hz.

J_{c0s}/J_{c0w} (1, 2, 5,10, 20, 50, 100). A pronounced peak in the $|\chi_3|$ curve at J_{c0s}/J_{c0w} = 1 can be observed. As the value of J_{c0s}/J_{c0w} increasing, more peaks, in $|\chi_3|$, $|\chi_5|$, $|\chi_7|$, $|\chi_9|$, appear, and the peak shift to higher temperatures and the peak heights decrease, shown in Fig. 5, which has been observed in experiments [12]. As for the magnitude of even harmonics as shown in Fig. 6, similar peaks as that in odd harmonics have been observed, however, it is interesting to note that the peak height shows opposite behavior, the peak heights in even harmonic curves increase with the increment of flux pinning ability.

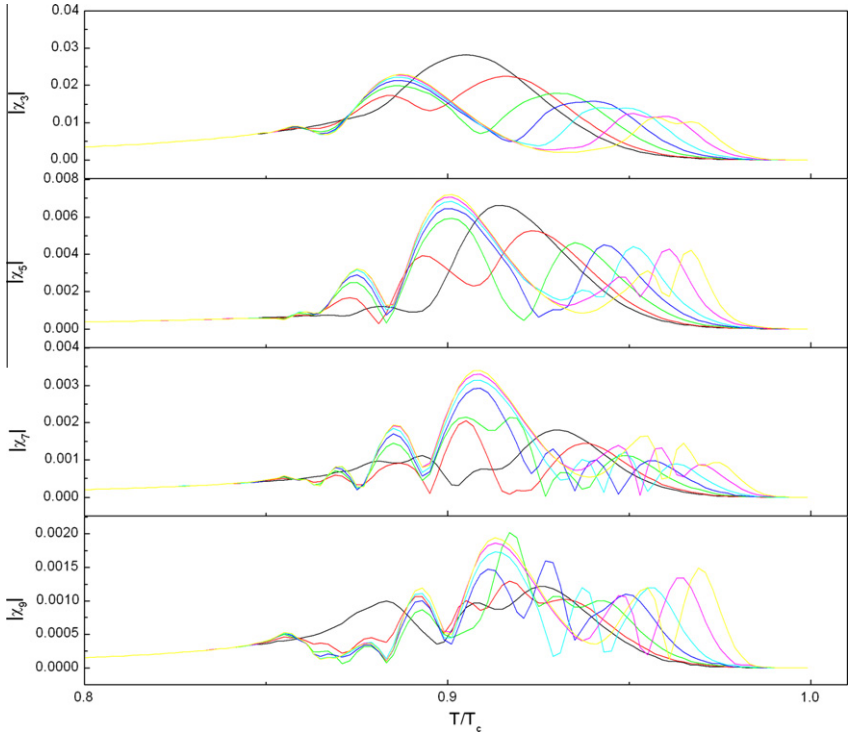

Fig. 5. The calculated curves of the magnitude of the odd harmonics $|\chi_n| = \sqrt{\chi_n'^2 + \chi_n''^2}$ ($n = 3, 5, 7, 9$) as a function of temperature with different J_{c0s}/J_{c0w}, as the arrows indicate: 1, 2, 5, 10, 20, 50, 100, for $B_{dc} = 0.05$ T, $B_{ac} = 0.5$ Gs, and $f = 500$ Hz.

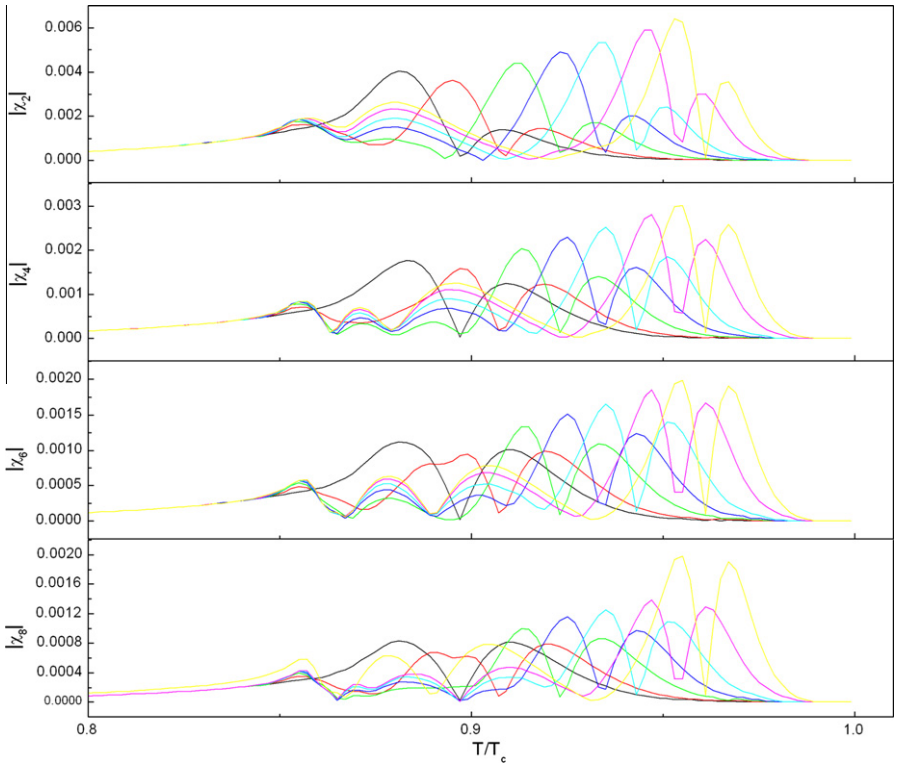

Fig. 6. The calculated curves of the magnitude of the even harmonics $|\chi_n| = \sqrt{\chi_n'^2 + \chi_n''^2}$ ($n = 2, 4, 6, 8$) as a function of temperature with different J_{c0s}/J_{c0w}, as the arrows indicate: 1, 2, 5, 10, 20, 50, 100, for $B_{dc} = 0.05$ T, $B_{ac} = 0.5$ Gs, and $f = 500$ Hz.

In order to display clearly the influence of different flux pinning ability in an intragrain on the harmonics, it is useful to plot χ'' as a function of χ' (Coles–Coles plot). Shown in Fig. 7, χ_3'' is plotted as a function of χ_3' at $B_{dc} = 0.05$ T, $B_{ac} = 0.5$ Gs, and $f = 500$ Hz for various values of J_{c0s}/J_{c0w} (1, 2, 5, 10, 20, 50, 100). In the case of $J_{c0s} = J_{c0w}$, a cardioids curve traversing the plot clockwise upon temperature

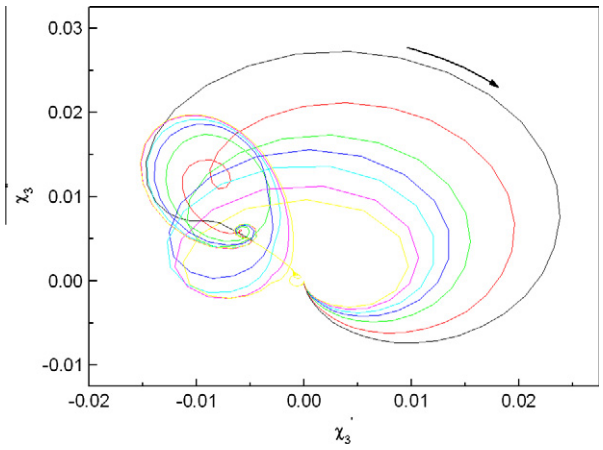

Fig. 7. Coles–Coles plot as obtained from the calculated temperature of χ_3.

increase can be observed. As the flux pinning ability of the intragrain enhances, the cardioids curves are distorted, and the closed areas get smaller. It may be used as a simple method to qualitatively estimate the values of J_{c0s}/J_{c0w}.

In polycrystalline high temperature superconductors, there exist the intergrain region (such as the weak links) and the intragrain region. As the flux pinning ability enhanced in the intragrain region, the characteristics in the complex susceptibility have been changed. As enhancement of flux pinning of intragrain region, two peaks come into being in fundamental AC susceptibility, and more peaks appear in the higher order even and odd harmonics. Moreover, the peaks at high temperatures move to higher temperature, and the peak heights increase in even harmonics, while, in odd harmonics the peak heights decrease with increasing flux pining of the intragrain. On the other hand, the Coles–Coles plot of χ_3 may be used to qualitatively estimate the values of J_{c0s}/J_{c0w}.

4. Conclusions

We have proposed a model to account for the effect of flux pinning ability of the intragrains characterized by critical current density on ACS in sintered superconductors. A sintered superconductor is described by alternating weak (intergrains or weak links) and strong (intragrains) regions depicted by different critical current densities J_{cw} and J_{cs}. Based on flux creep simulation, as the flux pinning ability enhanced in the intragrain region, a step and two peaks in fundamental AC susceptibility, and more peaks appear in the higher order even and odd harmonics, as reported in the references, are observed. The peaks at high temperatures move to higher temperature, and the peak heights increase in even harmonics, while, in odd harmonics the peak heights decrease with increasing flux pining of the intragrain. Moreover, the Coles–Coles plot of χ_3 may be used to qualitatively estimate the values of J_{c0s}/J_{c0w}.

Acknowledgments

This work was supported by the National Natural Science Foundation of China under Contract Nos. 11104001 and 50802096, the Foundation for the Excellent Youth Scholars of Anhui Education Office (No. 2010SQRL095), and the Scientific Research Foundation of the Anhui University of Architecture.

References

[1] F. Gömöry, Supercond. Sci. Technol. 10 (1997) 523.
[2] M. Yang, Y.H. Kao, Y. Xin, K.W. Wong, Phys. Rev. B 50 (1994) 13653.
[3] C.Y. Lee, Y.H. Kao, Physica C 241 (1995) 167.
[4] N. Yamada, T. Akune, N. Sakamoto, Y. Matsumoto, Physica C 412–414 (2004) 425.
[5] H. Jiang, C.P. Bean, Appl. Supercond. 2 (1994) 689.
[6] C.J. van der Beek, P.H. Kes, Phys. Rev. B 43 (1991) 13032.
[7] I.F. Voloshin, L.M. Fisher, V.S. Gorbachev, S.E. Savel'ev, V.A. Yampol'skii, JEPT Lett. 59 (1994) 55.
[8] L.M. Fisher, A.V. Kalinov, S.E. Savel'ev, I.F. Voloshin, V.A. Yampol'skii, Solid State Commun. 103 (1997) 313.
[9] D. Di Gioacchino, U. Gambardella, P. Tripodi, G. Grimaldi, Supercond. Sci. Technol. 16 (2003) 534.
[10] S. Dubois, F. Carmona, S. Flandrois, Physica C 260 (1996) 19.
[11] M.J. Qin, S.Y. Ding, H.M. Shao, X.X. Yao, Cryogenics 36 (1996) 619.
[12] A.J. Moreno, V. Bekeris, Physica C 329 (2000) 178.
[13] C. Senatore, M. Polichetti, D. Zola, T.D. Matteo, G. Giunchi, S. Pace, Physica C 388–389 (2003) 161.
[14] S.L. Shindé, J. Morrill, D. Goland, D.A. Chance, T. McGuire, Phys. Rev. B 41 (1990) 8838.
[15] T. Ishida, R.B. Goldfarb, Phys. Rev. B 41 (1990) 8937.
[16] L. Ji, R.H. Sohn, G.C. Spalding, C.J. Lobb, M. Tinkham, Phys. Rev. B 40 (1989) 10936.
[17] M.J. Qin, C.K. Ong, Phys. Rev. B 61 (2000) 9786.
[18] X.B. Xu, L. Zhang, X. Leng, S.Y. Ding, H.K. Liu, X.L. Wang, S.X. Dou, Z.W. Lin, J.G. Zhu, J. Appl. Phys. 97 (2005) 10B105.
[19] X. Leng, S.Y. Ding, Y. Liu, Z.H. Wang, H.K. Liu, S.X. Dou, Phys. Rev. B 68 (2003) 214511.
[20] L. Zhang, X. Leng, S.Y. Ding, X.B. Zhu, Y.P. Sun, Supercond. Sci. Technol. 23 (2010) 065020.
[21] L.M. Fisher, I.F. Voloshin, V.S. Gorbachev, S.E. Savel'ev, V.A. Yampol'skii, Physica C 245 (1995) 231.
[22] M.J. Qin, X.X. Yao, Phys. Rev. B 54 (1996) 7536.
[23] L.M. Fisher, K.V. Il'enko, A.V. Kalinov, M.A.R. LeBlanc, F. Perez-Rodrıguez, S.E. Savel'ev, I.F. Voloshin, V.A. Yampol'skii, Phys. Rev. B 61 (2000) 15382.